Sensors and Actuators B 252 (2017) 934–943

Contents lists available at ScienceDirect

Sensors and Actuators B: Chemical

journal homepage: www.elsevier.com/locate/snb

Research Paper

A molecular imprinting fluorescence sensor based on quantum dots and a mesoporous structure for selective and sensitive detection of 2,4-dichlorophenoxyacetic acid

Mengfan Jia[a], Zhong Zhang[a,*], Jinhua Li[b], Hongjun Shao[a], Lingxin Chen[b], Xingbin Yang[a,*]

[a] Shaanxi Engineering Laboratory for Food Green Processing and Safety Control, College of Food Engineering and Nutritional Science, Shaanxi Normal University, Xi'an 710119, China
[b] Key Laboratory of Coastal Environmental Processes and Ecological Remediation, Yantai Institute of Coastal Zone Research, Chinese Academy of Sciences, Yantai 264003, China

ARTICLE INFO

Article history:
Received 12 April 2017
Received in revised form 9 June 2017
Accepted 13 June 2017
Available online 15 June 2017

Keywords:
2,4-Dichlorophenoxyacetic acid
Molecular imprinting
Quantum dots
Mesoporous
Fluorescent detection

ABSTRACT

A novel molecular imprinting fluorescence sensor was constructed by anchoring mesoporous structured imprinting microspheres on the surfaces of quantum dots (QDs) surface for the selective and sensitive detection of 2,4-dichlorophenoxyacetic acid (2,4-D) on the basis of an electron-transfer-induced fluorescence quenching mechanism. The resulting sensor was well characterized and had ideal spherical morphology and fluorescence properties. Under the optimized conditions, the sensor exhibited a satisfactory linearity within 0.66–80 μM, with a low detection limit of 2.1 nM within 20 min. The sensor was successfully applied for the detection of 2,4-D in bean sprout samples, and high recoveries at three spiking levels of 2,4-D, ranging from 95.0 to 110.1%, with precisions below 4.9%, were attained. By taking advantage of surface imprinting and QDs, the sensor exhibited high sensitivity and good selectivity for the separation, enrichment and detection of 2,4-D in real food samples, thereby ensuring food safety.
© 2017 Elsevier B.V. All rights reserved.

1. Introduction

In a modern agricultural society, various herbicides, insecticides, and fungicides are commonly used at a large scale for the control of weeds, insects, and rodents, but some of these compounds have a detrimental effect on the ecosystem and human life, including carcinogenic or endocrine disrupting activities due to their accumulation in the food chain [1,2]. 2,4-D, which is a phenoxy compound, is commonly used in barley, wheat, corn and sorghum fields to control broad-leaf weeds [3]. As one of the top 10 pesticides, 2,4-D is used worldwide and has strong endocrine disrupting activities [4]. This compound is a pollutant of environmental concern and has been associated with the occurrence of cancer in humans, endocrine disruption, acute congestion, and degenerative changes in the central nervous system [5].

Conventional analytical methods, such as mass spectrometry [6], chromatography [7], electrochemistry [8] and colorimetric assays [9], are powerful tools that offer high sensitivity and specificity for the determination of pesticides; however, their associated high costs, complex sample pretreatment, and time-consuming labor requirements, as well as the low 2,4-D content in typical samples, impede their applications. Subsequently, several fast, cheap, and easy-to-use methods have been developed, including biosensors based on enzymes, aptamers or nucleic acids and enzyme-linked immunosorbent assays [10]. However, these methods require the isolation of other elements from the detected pesticides. Therefore, novel methods for highly effective detection of pesticides should be developed.

Fluorescence-based methods have potential applications in the detection of trace amounts of analytes because of their sensitivity, simplicity, and cost-effective features [11,12]. These methods are also considered to be feasible approaches to indicate the presence of an analyte, which induces a change in fluorescence color that is visible to the naked eye [13]. Organic dyes are often used as traditional fluorescent labels in fluorescence detection; however, these

Abbreviations: QD(s), quantum dot(s); 2,4-D, 2,4-dichlorophenoxyacetic acid; MIP(s), molecularly imprinted polymer(s); MES, 2-N-morpholinoethanesulfonic acid; APTES, 3-aminopropyltriethoxysilane; CTAB, cetyltrimethylammonium bromide; EDC, 3-ethylcarbodiimide hydrochloride; NHS, N-hydroxysuccinimide; SiO_2, Silica nanoparticles; TEM, transmission electron microscopy; BET, Brunauer–Emmett–Teller; BJH, Barrett–Joyner–Halenda; TG, thermogravimetry; DTG, derivative thermogravimetry; LUMO, lowest unoccupied molecular orbital; RSD, relative standard deviation; LOD, limit of detection.

* Corresponding authors.
E-mail addresses: zzhang@snnu.edu.cn (Z. Zhang), xbyang@snnu.edu.cn (X. Yang).

http://dx.doi.org/10.1016/j.snb.2017.06.090
0925-4005/© 2017 Elsevier B.V. All rights reserved.

dyes are easily photobleached and often exhibit narrow absorption and broad emission spectra with long tails, resulting in a low detection sensitivity [14]. By contrast, QDs are particularly attractive due to their good photostability, bright photoluminescence, high quantum yields, narrow emission, broad excitation, long fluorescence lifetimes, large extinction coefficients, and large Stokes Shifts [15,16]. QDs have been widely introduced as valid fluorescence probes in the analysis of metal ions [17], small molecules [18], and even biomacromolecules [19].

Another attractive material, molecularly imprinted polymers (MIPs), which are highly stable, easily prepared, and low cost, has been introduced for use in recognition to improve the selectivity of QDs-based probes and sensors [19,20]. This molecular imprinting technique (MIT) has been widely applied in various areas, including sample pretreatment [21], chromatographic separation [22], and chemical or biological sensing [23]. MIT is considered to be effective for the development MIP-based fluorescence sensors, which could combine the high selectivity of MIPs and high sensitivity of fluorescence detection [19]. However, MIPs prepared by traditional methods have numerous limitations, including incomplete template removal, small binding capacity, low affinity, and irregular material shapes [24]. Recently, MIPs on the surface of matrices have exhibited prominent properties. Surface imprinting is regarded as an effective technique to overcome material problems [25,26]. Subsequently, surface imprinting technique based on silica nanoparticles [27], magnetic Fe_3O_4 particles [28], nanotubes [29], polystyrene beads [30], and other materials, has been extensively investigated. Recently, surface imprinting of core-shell MIPs has been commonly applied and more widely used due to its intrinsic advantages, such as producing MIPs with good dispersion, better site accessibility, higher mass transfer, and easier and more completed template removal [31,32]. Among the support materials, silica nanoparticles are peculiarly prevalent for ameliorating the morphology of core-shell MIP particles. Moreover, mesoporous materials could enhance the selectivity of fluorescence sensors [33]. The use of mesoporous silica structured MIPs as selective recognition units and QDs as fluorescent detection units could improve sensitivity, response time, binding capacity and selectivity because of the large pore volumes and nanoscale pore wall thickness of the mesoporous structure and strong fluorescent signal of the QDs [34].

Inspired by these studies, we developed a simple, surface imprinting fluorescence sensor that used a QD-based mesoporous imprinted microsphere sensor strategy via sol-gel polymerization for the convenient, sensitive, and rapid recognition and detection of 2,4-D based on an electron-transfer-induced fluorescence quenching mechanism. QD-embedded silica nanoparticles act as the core of the support materials, and the mesoporous imprinted silica shell was deposited to fabricate the unique mesoporous MIP microsphere sensor, named SiO_2@QDs@m-MIPs. SiO_2@QDs@m-MIPs use CdTe QDs as fluorescence detection units and a mesoporous imprinted silica shell as highly selective recognition units. The sensor was well characterized, and its binding capacity, sensitivity, response time, stability, and selectivity were investigated systematically. Moreover, the sensor was successfully applied to complex food samples with satisfactory results, suggesting high potential for the specific recognition and accurate quantification of 2,4-D in complex matrices.

2. Experimental

2.1. Reagents and chemicals

2,4-D, carbendazol, tellurium powder, phenol, toluene, 2-*N*-morpholinoethanesulfonic acid (MES), 3-aminopropyltriethoxysilane (APTES), cetyltrimethylammonium bromide (CTAB), 3-ethylcarbodiimide hydrochloride (EDC), *N*-hydroxysuccinimide (NHS), cadmium nitrate ($Cd(NO_3)_2$), thioglycollic acid (TGA), and sodium borohydride ($NaBH_4$) were purchased from Sigma-Aldrich (Shanghai, China). High-performance liquid chromatography (HPLC)-grade methanol was purchased from TEDIA (Fairfield, OH, USA). All solvents, chemicals, and materials were at least of analytically pure grade and used directly without further purification unless otherwise specified. All aqueous solutions throughout this work were prepared using ultrapure water (18.2 MΩ specific resistance), which was prepared using a Millipore Milli Q-Plus system (Millipore, Bedford, MA, USA).

2.2. Synthesis of amino-functionalized SiO_2 nanoparticles

Silica nanoparticles (SiO_2) were synthesized based on the Stöber method and our previous experiment [35] with modifications. In brief, 30 mL of ethanol and 50 mL of ultrapure water were mixed, followed by the addition of 10 mL of $NH_3{\cdot}H_2O$. The mixture was magnetically stirred at room temperature for uniformity. Then, 7 mL of TEOS and 28 mL of ethanol were added dropwise with a constant-pressure dropping funnel, and the resultant mixture was stirred for 6 h. After 5 mL of APTES was added, the mixture reacted at room temperature for approximately 12 h with constant stirring. Then, the nanoparticles were separated from the reaction medium by centrifugation and washed several times with ethanol. The amino-functionalized SiO_2 nanoparticles were dispersed in 50 mL of ethanol for subsequent use.

2.3. Synthesis of carboxylated CdTe QDs

Carboxylated CdTe QDs were synthesized according to our previous report [36]. As a result, TGA-stabilized carboxylated CdTe QDs were attained.

2.4. Preparation of SiO_2@QDs

Nine milliliters of 20 mg/mL EDC in MES buffer (pH = 5.2, 0.1 mM) was mixed with a CdTe QD aqueous solution (15 mL) for 10 min. Then, 9 mL of 10 mg/mL NHS was added and mixed uniformly. Meanwhile, 5 mL of amino-functionalized SiO_2 particles was uniformly dispersed in 45 mL of MES buffer (pH = 5.2, 0.1 mM), followed by the addition of the above resultant QD solution dropwise. The mixture solution was stirred for 6 h at room temperature in the dark. Then, the obtained SiO_2@QDs composite nanoparticles were purified by repeated centrifugation at 7000 rpm for 10 min to remove the unbound QDs. As a result, SiO_2@QDs were obtained and dispersed in 50 mL of a PBS solution (0.01 M, pH 7.0).

2.5. Preparation of mesoporous MIPs (SiO_2@QDs@m-MIPs)

A 10 mL aliquot of a SiO_2@QDs nanoparticle solution was dispersed into 30 mL of ultrapure water. After ultrasonic vibration for 10 min, 160 μL of APTES and 37.78 mg of 2,4-D were added and stirred in the dark for 30 min. Then, 1.6 mL of CTAB (0.2 M) was added. After stirring for 30 min, 200 μL of $NH_3{\cdot}H_2O$ and 200 μL of TEOS were added into the mixture, and then, the mixture was stirred continuously for 12 h in the dark. The products were washed three times by using a mixed solvent of ethanol/0.001 M HCl (8:2, v/v) to remove 2,4-D and CTAB and then dried in a vacuum oven at 40 °C. Finally, mesoporous products were obtained and named SiO_2@QDs@m-MIPs (MIPs, for simplicity). In addition, mesoporous nonimprinted polymers, that is, SiO_2@QDs@m-NIPs (NIPs, for simplicity), were prepared via the same procedure, but without the addition of the template 2, 4-D.

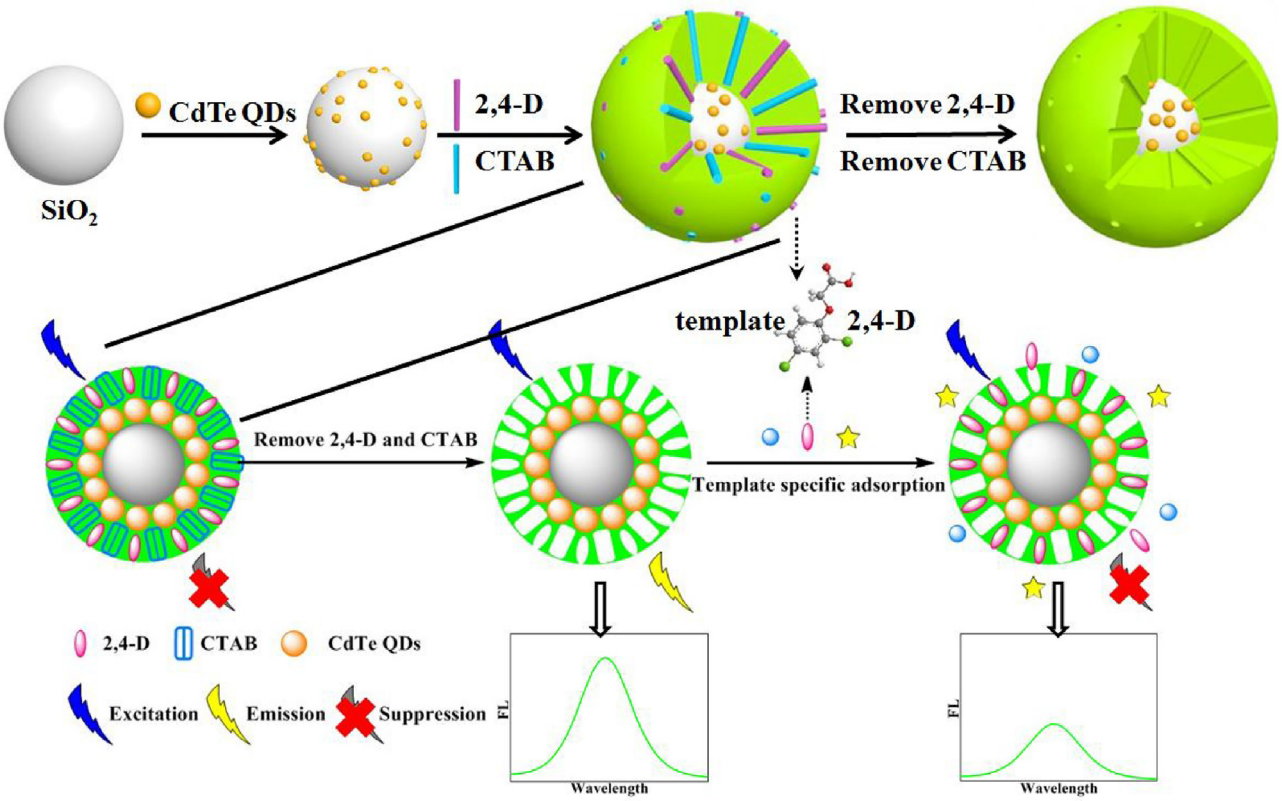

Fig. 1. Schematic of the process for the preparation of SiO_2@QDs@m-MIPs.

2.6. Characterization

Morphological evaluation was performed by transmission electron microscopy (TEM, HT-7700, operated at 80 kV). N_2 adsorption-desorption isotherms and structural parameters were determined via Brunauer-Emmett–Teller (BET) analysis by Fully Automatic Specific Surface Instruments (ASAP 2020, Beishide Instruments). Fourier Infrared spectra (FT-IR) were obtained using an infrared spectrometer (Tensor 27, Bruker) to examine the preparation process. Fluorescence spectra were recorded using a spectrofluorometer (Thermo): the excitation light was set at 350 nm, emission spectra were measured from 370 nm to 670 nm for 2,4-D, and slit widths of excitation and emission were set at 5 nm and 5 nm, respectively. The amount of 2,4-D adsorbed onto the imprinted polymer shells was determined by measuring the difference between the total 2,4-D amount and residual amount in solution using HPLC-UV. For the HPLC-UV procedure, a C_{18} column (4.6 mm i.d. × 250 mm, 5 μm, Venusil, USA) was used as the analytical column. The HPLC conditions optimized for 2,4-D were as follows: mobile phase, methanol-water (6:4, v/v); flow rate, 1.0 mL min^{-1}; room temperature; UV detection, 285 nm for 2,4-D; and injection volume, 20 μL.

2.7. Analysis of real samples

Bean sprout samples, including soybean sprout and mung bean sprout juice, were utilized to examine the practical applicability of SiO_2@QDs@m-MIPs for 2,4-D detection. Bean sprout juice was collected from the bean sprout medium, and the samples were filtered using a 0.45 μm microfiltration membrane to remove any possible suspended particles before use and then diluted 100-fold for spiking. Spiked samples with known concentrations of 2,4-D were used to validate the accuracy and application of the SiO_2@QDs@m-MIPs sensor.

3. Results and discussion

3.1. Preparation of SiO_2@QDs@m-MIPs

The preparation and imprinting process of SiO_2@QDs@m-MIPs is schematically illustrated in Fig. 1. In the first step, SiO_2 nanoparticles were used as core support materials, and abundant CdTe QDs were introduced to the surface of the amino-functionalized SiO_2 core by amide bonding. Subsequently, the imprinted silica shell on the surface of SiO_2@QDs was formed in the course of the second-stage mini-emulsion polymerization with APTES, TEOS, $NH_3 \cdot H_2O$, and CTAB as the functional monomer, cross-linker, catalyst, and surfactant, respectively. Finally, specific imprinted cavities and mesoporous structures of SiO_2@QDs@m-MIPs were obtained after removing the template 2,4-D and surfactant CTAB. Compared with the complex surface modification for the general preparation of MIPs, this m-MIPs silica shell layer not only facilitated high accessibility to binding sites and rapid mass transfer of template molecules but also protected the fluorescence of the QDs and effectively decreased the QDs toxicity. The obtained SiO_2@QDs@m-MIPs enabled the easy recognition, separation, and enrichment of 2,4-D from complex food samples. With the use of SiO_2@QDs@m-MIPs to detect 2,4-D, a Meisenheimer complex was produced on the surface of the QDs between 2,4-D and the primary amino groups. Then, the photoluminescent energy of the QDs was transferred to the complex and resulted in QD fluorescence quenching. Therefore, the obtained SiO_2@QDs@m-MIPs facilitated the easy recognition, separation, and enrichment of 2,4-D from complex food samples.

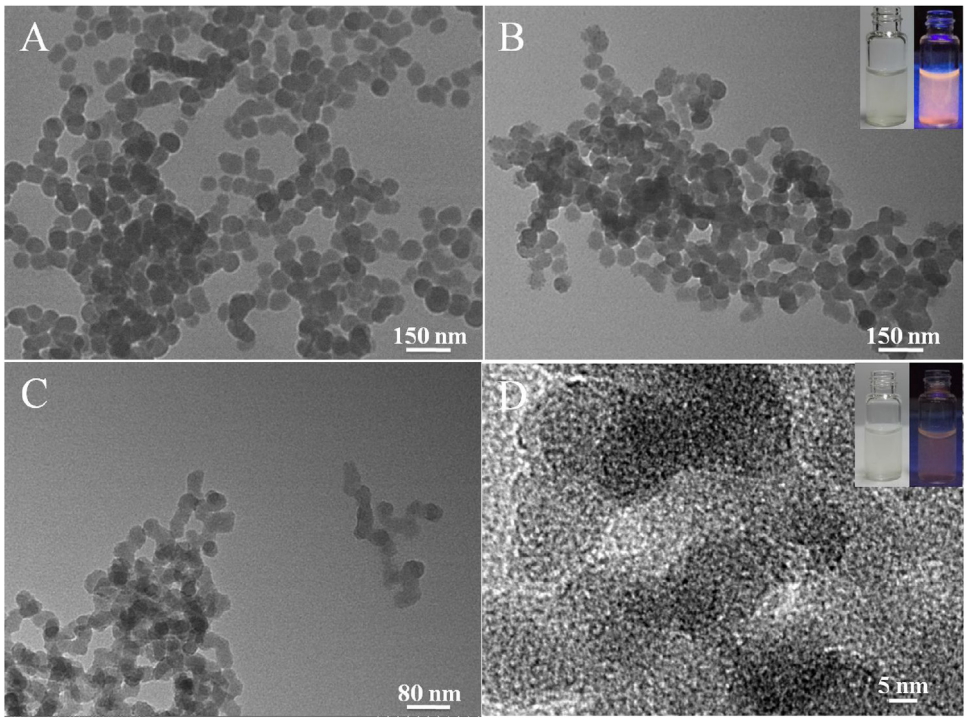

Fig. 2. (A) TEM image of SiO_2, (B) TEM image of SiO_2@QDs, and (C,D) TEM images of SiO_2@QDs@m-MIPs. (Inset of B: photographs of SiO_2@QD solution under sunlight (left) and ultraviolet lamps (right), inset of D: photographs of SiO_2@QDs@m-MIP solution under sunlight (left) and ultraviolet lamps (right)).

3.2. Characterization of SiO_2@QDs@m-MIPs

The morphologies of SiO_2, SiO_2@QDs and SiO_2@QDs@m-MIPs were characterized by TEM. SiO_2 nanoparticles (Fig. 2A) exhibited good dispersion and a diameter of approximately 50–80 nm, and SiO_2@QDs nanoparticles (Fig. 2B) displayed good dispersion and smooth surfaces, with an average diameter of 50–80 nm. As shown in Fig. 2C and D, m-MIPs exhibited similar morphologies; the rough surfaces of m-MIPs and worm-like channels indicated the existence of a shell and the mesoporous structures. In addition, the mesoporous structures of the m-MIPs and m-NIPs were further examined by BET analysis, and the obtained specific surface areas of m-MIPs and m-NIPs were 127.6 and 139.4 m^2/g, respectively. As shown in Fig. S1A and S1B, the N_2 sorption isotherm of the m-MIPs and m-NIPs showed a rapid increase in the adsorption branch at a relative pressure of 0.4–0.6, clearly indicating considerable numbers of uniform mesopores in the m-MIPs. These uniform mesopores of the m-MIPs possessed an average diameter of 3.95 nm, as obtained from the Barrett-Joyner-Halenda (BJH) pore size distribution curve (Fig. S1C). This mesoporous structure markedly decreased mass-transport resistance, provided easier accessibility, and improved the recognition sites. These results prove that binding cavities were formed on the surface of m-MIPs by the template molecules.

The FT-IR of the samples are shown in Fig. 3. The wide, strong absorption band at approximately 1091 cm^{-1} is attributed to the asymmetric stretching vibrations of Si—O—Si, and the peaks at approximately 466 and 794 cm^{-1} are ascribed to the Si-O antisymmetric stretching vibration (Fig. 3a). These characteristic peaks were evident in the three FT-IR spectra, indicating the occurrence of SiO_2 matrices in the three materials. Meanwhile, the stretching vibrations of N—H at 1631 and 3436 cm^{-1} reveal that the amino group was modified on the surface of SiO_2 nanoparticles. As shown in Fig. 3b and c, the enhanced absorption peak at approximately 1411 cm^{-1} is assigned to the C—N stretching vibration of the acylamino group, thereby suggesting the successful grafting of QDs on SiO_2. As displayed in Fig. 3c, SiO_2@QDs@m-MIPs did not show other characteristic peaks; however, the characteristic absorption peaks for SiO_2 and the acylamino group were significantly weakened, suggesting that a thin imprinted shell layer was successfully modified on the surface of the SiO_2@QDs particles.

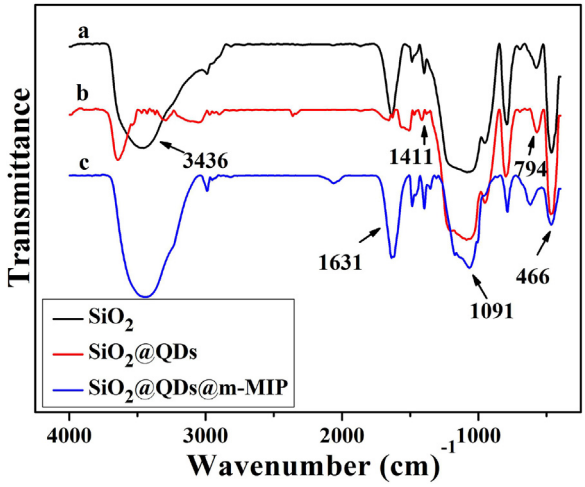

Fig. 3. FT-IR spectra of (a) SiO_2, (b) SiO_2@QDs, and (c) SiO_2@QDs@m-MIPs.

The thermogravimetry (TG) and derivative thermogravimetry (DTG) curves of the m-MIPs and m-NIPs are shown in Fig. S2A and S2B. With the increase in temperature from 25 to 100 °C, the weight loses of the m-MIPs and m-NIPs are mainly due to the volatile loss of absorbed water. As shown in Fig. S2, the weight of the m-MIPs suffered a sharper decrease than that of the m-NIPs possibly because of the existence of more pores on the surface of the m-MIPs compared to the m-NIPs; these pores can absorb more water molecules before 100 °C. In the range of 100–460 °C, the weight losses of the m-MIPs

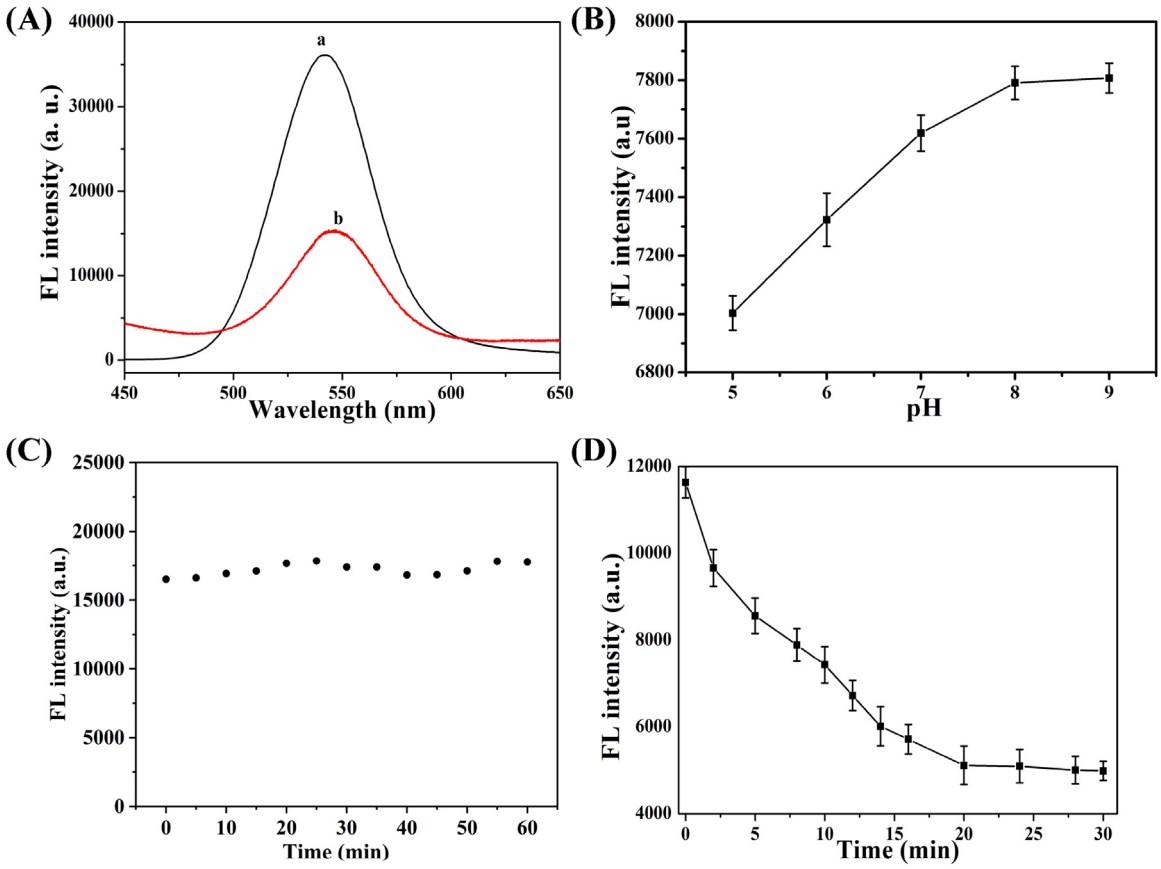

Fig. 4. (A) Fluorescence spectra of (a) QDs and (b) SiO_2@QDs@m-MIPs. (B) Effect of pH on the fluorescence intensity of SiO_2@QDs@m-MIPs. (C) Fluorescence intensity of SiO_2@QDs@m-MIP solution within 60 min. (D) Fluorescence response time of SiO_2@QDs@m-MIPs.

and m-NIPs were extremely slow, suggesting that the stabilities of both particles were below 460 °C. By contrast, the higher weight loss rates of the m-MIPs and m-NIPs observed at temperatures ranging from 460 to 650 °C may have resulted from the dissolution of the MIPs [37]. The peak temperature levels of the m-MIPs and m-NIPs were both at 580 °C, and the residual amounts of m-MIPs and m-NIPs were 70.5 and 81.5%, respectively. Therefore, we can conclude that the prepared m-MIPs and m-NIPs have excellent thermal stability at temperatures lower than 460 °C. This was also clearly observed from the DTG curve.

3.3. Binding properties of the SiO_2@QDs@m-MIPs for 2,4-D

To estimate the binding performances of the m-MIPs and m-NIPs, we conducted adsorption capacity analysis by using 0.1 mg/mL of 2,4-D through HPLC-UV analysis. As shown in Fig. S3, the adsorption capacity of the MIPs is 1.50 mg/g, which is considerably larger than that of the NIPs (0.50 mg/g), indicating that abundant specific binding sites are obtained during the MIP preparation procedure after the removal of the template molecules. Therefore, the m-MIPs can be applied as ideal adsorption materials for the selective recognition and determination of 2,4-D.

3.4. Fluorescence properties of the SiO_2@QDs@m-MIPs

In this work, QDs were buried under the thin mesoporous imprinted silica layer after MIP shell encapsulation. Our previous study demonstrated that encapsulated QDs retained their fluorescence properties while the emission peak showed a slight red shift [36], which is consistent with this work (Fig. 4A). Therefore, we conclude that SiO_2@QDs@m-MIPs have good fluorescence properties. Moreover, the suitable excitation wavelength was tested in this work, and the results are shown in Fig. S4.

In addition, the acidity of the solution plays a key part in the fluorescence property because of its significant impact on the three-dimensional structures, charge of 2,4-D, the fluorescence intensity of SiO_2@QDs@m-MIPs. Thus, acidity influenced the rebinding of 2,4-D at different pH values. Fig. 4B shows the effects of pH on the fluorescence intensity change of MIPs. The fluorescence intensity was low at pH values below 7.0; however, the fluorescence intensity increased with an increase of pH from 5.0 to 7.0. At pH levels higher than 7.0, the fluorescence intensity increased more slowly as the pH value increased, and the fluorescence intensity became virtually steady at pH 8.0. Considering the good fluorescence intensity and possible applications of MIPs in food samples, we selected pH 7.0 as the appropriate level for subsequent experiments.

Accordingly, the fluorescence stability of m-MIPs was estimated by repeated detection of the fluorescence intensity every 10 min at the maximum emission peak. As shown in Fig. 4C, the fluorescence intensity of the m-MIPs was virtually unchanged within 60 min, revealing that the m-MIPs have good physical stability and chemical inertness because of the core-shell structure. Furthermore, for storage stability, repeated detection of the fluorescence intensity was recorded every week, and intensity remained at 94.3% of the original intensity, indicating that the fluorescence sensor has satisfactory storage stability. Moreover, the m-MIPs sensor still provided nearly equivalent detection results after storage at 4 °C for two months. These results suggest that the MIP silica shell protects the QDs well.

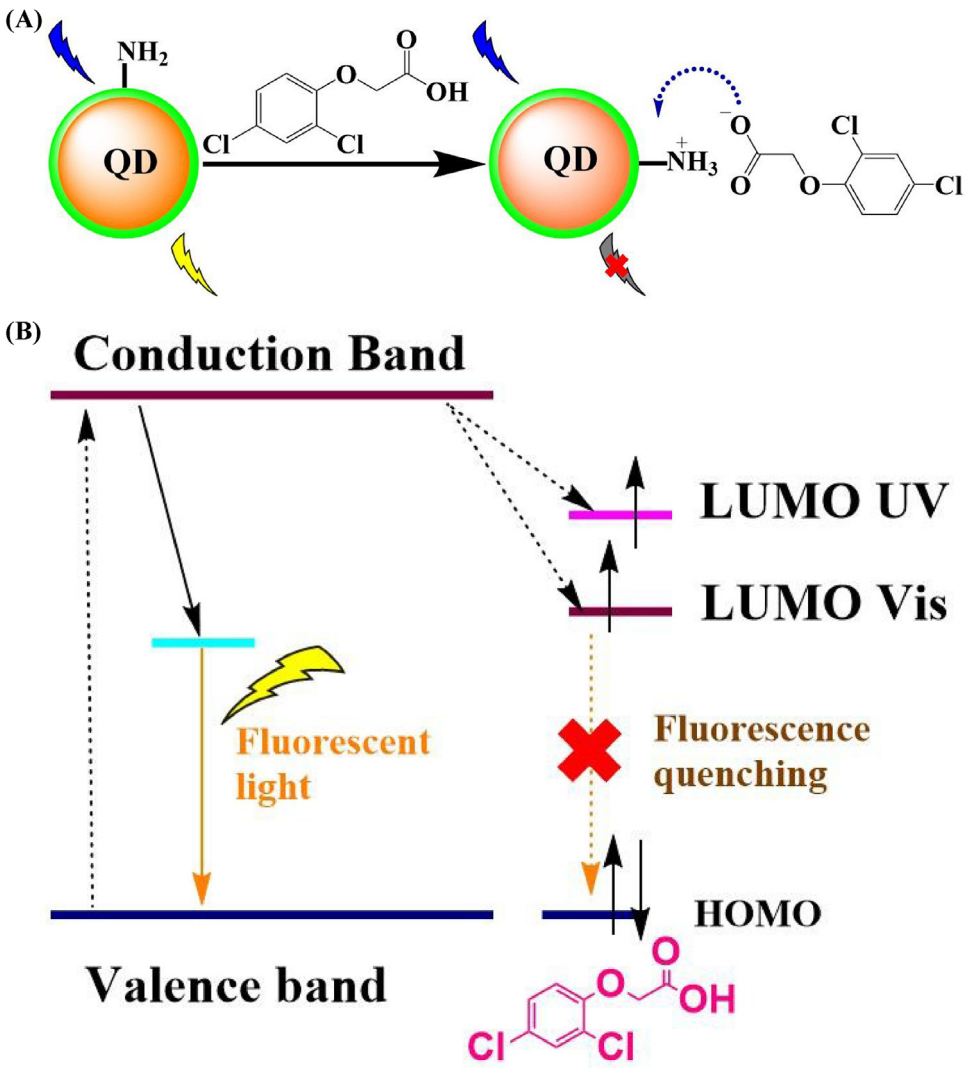

Fig. 5. (A) Schematic for the QDs fluorescence quenching mechanism based on electron-transfer-induced energy transfer. (B) Schematic of molecular orbital theory for the fluorescence quenching mechanism.

To evaluate the accessibility to binding sites, the response time of this sensor was tested. As shown in Fig. 4D, at a template 2,4-D concentration of 50 μM in the m-MIPs, the fluorescence intensity at 540 nm decreased rapidly within 20 min, after which the curve reached equilibrium. The recognition sites among the pores of the mesoporous structure offered rapid mass transfer and high recognition accessibility toward 2,4-D, resulting in a rapid response speed for the template molecule. Therefore, 20 min was selected as the response time for further study.

3.5. Possible detection mechanism of the SiO_2@QDs@m-MIPs

The prepared SiO_2@QDs@m-MIPs were used to recognize and detect 2,4-D, and the process is schematically illustrated in Fig. 1. A strong charge-transfer interaction reportedly occurs between this electron-rich aromatic ring (conjugating OH) and electron-deficient amino group. Herein, as shown in Fig. 5A, electron transfer from the carboxyl groups to the amino groups led to the formation of a Meisenheimer complex between the radical amino groups and 2,4-D on the surface of the QDs. Afterward, the energy of the QDs was transferred to the complex, leading to QD fluorescence quenching. Thus, the fluorescence of 2,4-D was detected. Moreover, as shown in Fig. 5B, the quenching mechanism could be expounded on by molecular orbital theory. The electrons of the QDs are able to accept the UV energy and then become excited from the valence band to the conduction band. Subsequently, the excited electron returns to the ground state. During the return course, QDs emit fluorescence (Fig. 5B). In addition, a hydrogen bond forms between 2,4-D and the primary amino groups on the surface of the QDs after the addition of 2,4-D, and the strong interaction force results in electron transfer between the QDs and 2,4-D.

The UV absorption of 2,4-D is at approximately 285 nm, which is close to the conduction band of the CdTe QDs; therefore, electrons excited to the conduction band could directly jump to the ultraviolet and visible energy levels of the lowest unoccupied molecular orbital (LUMO) of 2,4-D, as indicated by the arrows in Fig. 5B. All of the energy of 2,4-D is higher than that of CdTe QDs at approximately 540 nm; therefore, the excited electrons returned to the ground state in the manner shown by the dotted line in Fig. 5B, resulting in fluorescence quenching of the QDs. According to the above explanation of the detection mechanism, when more template molecules are adsorbed onto the surface of the core-shell microspheres, greater fluorescence quenching will be initiated and the quenching constant will remain constant, indicating that the con-

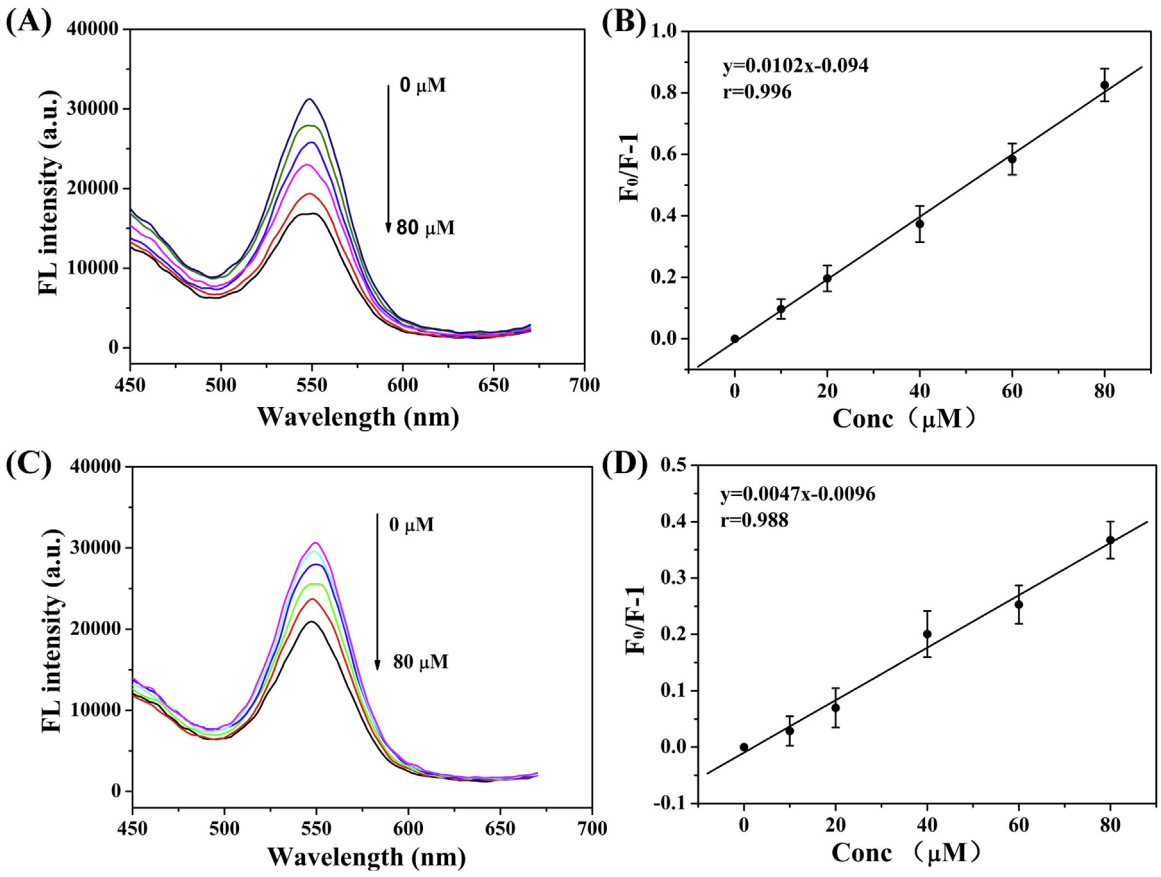

Fig. 6. (A, B) Fluorescence emission spectra of SiO_2@QDs@m-MIPs and SiO_2@QDs@m-NIPs with the addition of the indicated concentrations of 2,4-D, respectively. (C, D) Corresponding fluorescence intensity Stern-Volmer plots of SiO_2@QDs@m-MIPs and SiO_2@QDs@m-NIPs.

centration of 2,4-D is positively correlated with the fluorescence quenching value. Thus, 2,4-D could be detected by fluorescence.

3.6. Sensitivity and selectivity of the sensor

The quality of the SiO_2@QDs@m-MIPs fluorescent sensor for the quantitative determination of 2,4-D was further evaluated. Under the optimized parameters, the fluorescence spectra of the mesoporous fluorescence m-MIPs sensor at different concentrations of 2,4-D were examined to determine their sensitivity. As shown in Fig. 6A, the fluorescence intensities clearly decreased with the increase in 2,4-D concentrations and linearity was presented within a wide range of 0.66–80 μM, with a correlation coefficient of 0.996 (Fig. 6B). In addition, a favorable limit of detection (LOD, S/N = 3) of 2.1 nM was obtained and could be applied to trace analysis. Also, as shown in Fig. 6C, the fluorescence intensity of m-NIPs could be quenched by the addition of 2,4-D; however, the linear range was narrow, and the decrease of fluorescence intensity of the corresponding m-NIPs was not obvious at the same 2,4-D concentration. This phenomenon can be explained by the absence of specific recognition sites in m-NIPs; therefore, 2,4-D could not enter the inner of the m-NIPs and only the fluorescence intensity of the QDs located on the surface of m-NIPs were able to be quenched, with most QDs remaining steady [38]. Thus, this m-MIPs sensor detected 2,4-D with good sensitivity and selectivity, indicating the feasibility of the sensor for determining 2,4-D residues in food samples.

Accordingly, the fluorescence quenching in this system followed the Stern-Volmer equation as follows:

$$F_0/F = 1 + K_{SV}C_q$$

where F_0 and F are the fluorescent intensities in the absence and presence of quencher, respectively; K_{SV} is the quenching constant for the quencher; and C_q is the concentration of the quencher. The ratio of $K_{sv,m\text{-}MIP}$ to $K_{sv,m\text{-}NIP}$ is defined as the imprinting factor, and $(F_0/F)-1$ is defined as the quenching amount. In general, fluorescence quenching includes two quenching modes, namely, dynamic and static quenching. In this work, the absorption spectra of SiO_2@QDs@m-MIPs were measured to determine the quenching mechanism. The absorption spectra of SiO_2@QDs@m-MIPs changed with the addition of the quencher; thus, we concluded that fluorescence quenching occurred as static quenching. As shown in Fig. 6A and C, m-MIPs and m-NIPs displayed different Stern-Volmer plot relationships and the decrease in fluorescence intensity of the m-MIP coated QDs was substantially larger than that of the m-NIP coated QDs at the same concentration of 2,4-D. In addition, an imprinting factor of 2.17 was obtained.

By contrast, the selectivity of the m-MIPs sensor was evaluated by recording the fluorescence emission of the sensor in the presence of 2,4-D and its structurally similar compounds, including phenol, toluene, and carbendazol. As shown in Fig. 7, the m-MIP sensor displayed a significant change in fluorescence quenching toward 2,4-D, which was considerably larger than that of its analogs; this change was possibly caused by the extremely close and relatively low fluorescence quenching. This difference is likely due to the difference in molecular weight, spatial structure, and interaction with APTES between 2,4-D and its analogs. Therefore, the MIPs sensor possesses high selectivity toward the template molecule 2,4-D.

Table 1
Spiked recoveries and relative standard deviations (RSD, %, $n = 3$) for the determination of 2,4-D in bean sprout samples using the SiO_2@QDs@m-MIPs and HPLC-UV analysis.

Sample	Spiked (μmol/L)	SiO_2@QDs@m-MIPs		HPLC results
		Found (μmol/L)	Recovery ± RSD (%)	Found (μmol/L)
Soybean sprout	0	0	–	–
	5	4.81	96.2 ± 4.9	4.96
	10	10.4	104.2 ± 4.5	9.89
	20	21.5	107.5 ± 4.1	20.9
Mung bean sprout	0	0	–	–
	5	4.82	96.4 ± 4.8	4.93
	10	9.51	95.0 ± 4.6	10.1
	20	22.0	110.1 ± 3.9	19.6

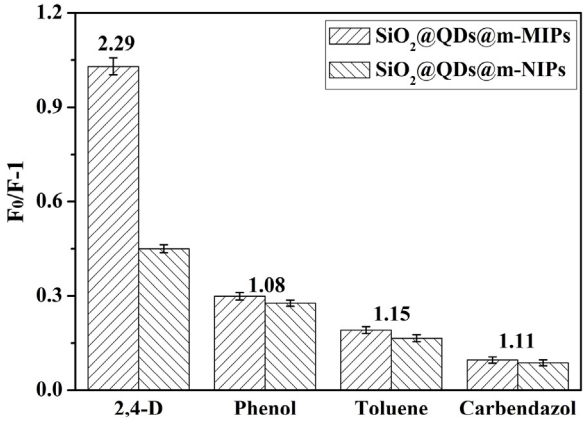

Fig. 7. Selectivity of the mesoporous SiO_2@QDs@m-MIPs and SiO_2@QDs@m-NIPs to other template analog (2,4-D, phenol, toluene, and carbendazol) solutions at the same concentration.

3.7. Practical application of the sensor to real samples

To further assess the applicability of the SiO_2@QDs@m-MIPs sensor, the detection of 2,4-D in bean sprout juice samples was rigorously evaluated by recovery tests. The average recovery was acquired with the relative standard deviation (RSD) based on three triplicate measurements for each concentration. As listed in Table 1, the recoveries of 2,4-D were statistically approximate to those of the spiked values, indicating the absence of severe positive or negative interferences in real food samples. Moreover, satisfactory recoveries of 96.2–107.5% with RSDs of 4.1–4.5% were obtained for the spiked soybean sprout samples, respectively, and 95.0–110.1% with RSDs of 3.9–4.8% were achieved for the mung bean sprout juice samples. In addition, this experiment confirmed that the data were in agreement with those obtained by the HPLC method (Table 1). Overall, the results indicate that the SiO_2@QDs@m-MIPs sensor possesses considerable potential for the practical detection of 2,4-D in real food samples.

3.8. Method performance comparison

The performance of the developed SiO_2@QDs@m-MIPs method for the detection of 2,4-D was compared with several reported MIP-based methods, as listed in Table S1. As shown in the table, most reported MIP-based methods presented long [39,40] or uncertain [41–43,45] response time, meaning that these methods require sophisticated sample treatment and long analysis times. Moreover, the LODs for some methods were not clear or the methods were not applied in real samples [42–44]. Yu et al. [46] reported a paper-based MIP-grafted multi-disk micro-disk plate for the sensitive and specific chemiluminescence detection of 2,4-D with a response time of only 4 min. However, time-consuming synthesis and hard control performance restricted its application. Our developed SiO_2@QDs@m-MIPs sensor system required no complicated sample pretreatment or costly instruments, and this system demonstrated high sensitivity and selectivity as well as rapid response for the fluorescent detection to 2,4-D. In our study, the ultrathin imprinting shell layer was anchored on the surface of CdTe QDs via a surface imprinting process. Moreover, the mesoporous structure played a key role in response rapidity and sensitivity improvement. As a result, SiO_2@QDs@m-MIPs presented high sensitivity and selectivity, a short analysis time, as well as good reliability and applicability.

4. Conclusions

Based on electron-transfer-induced fluorescence quenching, a sol-gel core-shell imprinting approach for the convenient, selective recognition and highly sensitive detection of 2,4-D in real food samples was successfully developed by fabricating a mesoporous SiO_2@QDs@m-MIPs sensor. In the presence of 2,4-D, the fluorescence intensity of the m-MIPs sensor was weakened due to electron transfer. By taking advantage of the synergy of the high selectivity of the MIPs and excellent fluorescence property of the QDs, the SiO_2@QDs@m-MIPs sensor demonstrated highly selective and sensitive recognition and determination of 2,4-D. Moreover, the obtained sensor exhibited reproducibility, responsiveness, repeatability, and stability. The sensor can be utilized as an alternative analytical tool for 2,4-D and is expected to present strong potential in the routine monitoring of food quality control and market surveillance to ensure food supply safety. Furthermore, more efforts should be focused on the development of QDs@m-MIP-based sensors with improved performances. The combination of imprinting technology, signal units (such as QDs), and core-shell polymers opens a new window of interest in the exploration of functionalized polymers and provides new opportunities for applications involving the highly selective recognition of targeted species.

Acknowledgements

This work was financially supported by the National Natural Science Foundation of China (31671823, 21477160), Shanxi Province Agricultural Science and Technology Innovation and Key Project (2016NY-181, 2016NY-174), the Fundamental Research Funds for the Central Universities in China (GK201603099, GK201501006).

Appendix A. Supplementary data

Supplementary data associated with this article can be found, in the online version, at http://dx.doi.org/10.1016/j.snb.2017.06.090.

References

[1] S. Buranatrevedh, D. Roy, Occupational exposure to endocrine-disrupting pesticides and the potential for developing hormonal cancers, J. Environ. Health 64 (2001) 17–29.
[2] J. He, L.X. Song, S. Chen, Y.Y. Li, H.L. Wei, D.X. Zhao, K.R. Gu, S.S. Zhang, Novel restricted access materials combined to molecularly imprinted polymers for selective solid-phase extraction of organophosphorus pesticides from honey, Food Chem. 187 (2015) 331–337.
[3] A. Boivin, S. Amellal, M. Schiavon, M.T. van Genuchten, 2, 4-Dichlorophenoxyacetic acid (2, 4-D) sorption and degradation dynamics in three agricultural soils, Environ. Pollut 138 (2005) 92–99.
[4] S.M. Wang, L. Ge, L. Li, M. Yan, S.G. Ge, J.H. Yu, Molecularly imprinted polymer grafted paper-based multi-disk micro-disk plate for chemiluminescence detection of pesticide, Biosens. Bioelectron. 50 (2013) 262–268.
[5] K.V. Gobi, H. Tanaka, Y. Shoyama, N. Miura, Highly sensitive regenerable immunosensor for label-free detection of 2,4-dichlorophenoxyacetic acid at ppb levels by using surface plasmon resonance imaging, Sens. Actuators B 111–112 (2005) 562–571.
[6] A.P. Deng, H.T. Liu, S.J. Jiang, H.J. Huang, C.W. Ong, Reaction cell inductively coupled plasma mass spectrometry-based immunoassay using ferrocene tethered hydroxysuccinimide ester as label for the determination of 2,4-dichlorophenoxyacetic acid, Anal. Chim. Acta 472 (2002) 55–61.
[7] J.A. Oh, H.S. Shin, Simple determination of hydrazine in waste water by headspace solid-phase micro extraction and gas chromatography-tandem mass spectrometry after derivatization with trifluoro pentanedione, Anal. Chim. Acta 950 (2017) 57–63.
[8] S. Viswanathan, H. Radecka, J. Radecki, Electrochemical biosensor for pesticides based on acetylcholinesterase immobilized on polyaniline deposited on vertically assembled carbon nanotubes wrapped with ssDNA, Biosens. Bioelectron. 24 (2009) 2772–2777.
[9] M. Pohanka, J.Z. Karasova, K. Kuca, J. Pikula, O. Holas, J. Korabecny, J. Cabal, Colorimetric dipstick for assay of organophosphate pesticides and nerve agents represented by paraoxon, sarin and VX, Talanta 81 (2010) 621–624.
[10] I.B. Tahirbegi, J. Ehgartner, P. Sulzer, S. Zieger, A. Kasjanow, M. Paradiso, M. Strobl, D. Bouwes, T. Mayr, Fast pesticide detection inside microfluidic device with integrated optical pH, oxygen sensors and algal fluorescence, Biosens. Bioelectron. 88 (2017) 188–195.
[11] L. Yuan, W. Lin, K. Zheng, L. He, W. Huang, Far-red to near infrared analyte-responsive fluorescent probes based on organic fluorophore platforms for fluorescence imaging, Chem. Soc. Rev. 42 (2013) 622–661.
[12] H.N. Kim, W.X. Ren, J.S. Kim, J.Y. Yoon, Fluorescent and colorimetric sensors for detection of lead cadmium, and mercury ions, Chem. Soc. Rev. 41 (2012) 3210–3244.
[13] H.J. Zhu, T. Yu, H.D. Xu, K. Zhang, H. Jiang, Z.P. Zhang, Z.Y. Wang, S.H. Wang, Fluorescent nanohybrid of gold nanoclusters and quantum dots for visual determination of lead ions, ACS Appl. Mater. Interfaces 6 (2014) 21461–21467.
[14] U.R. Genger, M. Grabolle, S. Cavaliere-Jaricot, R. Nitschke, T. Nann, Quantum dots versus organic dyes as fluorescent labels, Nat. Methods 5 (2008) 763–775.
[15] L. Zhu, X. Cui, J. Wu, Z. Wang, P. Wang, Y. Hou, M. Yang, Fluorescence immunoassay based on carbon dots as labels for the detection of human immunoglobulin G, Anal. Methods 6 (2014) 4430–4436.
[16] A. Valizadeh, H. Mikaeili, M. Samiei, S.M. Farkhani, N. Zarghami, M. Kouhi, A. Akbarzadeh, S. Davaran, Quantum dots: synthesis, bioapplications, and toxicity, Nanoscale Res. Lett. 7 (2012) 480–494.
[17] J.L. Chen, A.F. Zheng, Y.C. Gao, C.Y. He, G.H. Wu, Y.C. Chen, X.M. Kai, C.Q. Zhu, Functionalized CdS quantum dots-based luminescence probe for detection of heavy and transition metal ions in aqueous solution, Spectrochim. Acta, Part A 69 (2008) 1044–1052.
[18] H.D. Chen, Y.S. Xia, Compact hybrid (gold nanodendrite-quantum dots) assembly: plasmon enhanced fluorescence-based platform for small molecule sensing in solution, Anal. Chem. 86 (2014) 11062–11069.
[19] Y.X. Ma, S.Y. Xu, S.G. Wang, L.Y. Wang, Luminescent molecularly-imprinted polymer nanocomposites for sensitive detection, TrAC, Trends Anal. Chem. 67 (2015) 209–216.
[20] H.L. Liu, X.M. Chen, L. Mu, J. Wang, B.G. Sun, Application of quantum dot-molecularly imprinted polymer core- shell particles sensitized with graphene for optosensing of Nε-carboxymethyllysine in dairy products, J. Agric. Food Chem. 64 (2016) 4801–4806.
[21] F. Tang, Q.W. Yu, B.F. Yuan, Y.Q. Feng, Hydrophilic materials in sample pretreatment, TrAC, Trends Anal. Chem. 86 (2017) 172–184.
[22] H.Y. Zong, X. Liu, Z.S. Liu, Y.P. Huang, Molecular crowding-based imprinted monolithic column for capillary electrochromatography, Electrophoresis 36 (2015) 818–824.
[23] B.B. Prasad, S. Jaiswal, K. Singh, Ultra-trace analysis of d-and l-aspartic acid applying one-by-one approach on a dual imprinted electrochemical sensor, Sens. Actuators B 240 (2017) 631–639.
[24] X.Y. Wang, Q. Kang, D.Z. Shen, Z. Zhang, J.H. Li, L.X. Chen, Novel monodisperse molecularly imprinted shell for estradiol based on surface imprinted hollow vinyl-SiO_2 particles, Talanta 124 (2014) 7–13.
[25] X.L. Hu, X. Wu, F.F. Yang, Q. Wang, C.Y. He, S.R. Liu, Novel surface dummy molecularly imprinted silica as sorbent for solid-phase extraction of bisphenol A from water samples, Talanta 148 (2016) 29–36.
[26] Z. Zhang, J.H. Li, L.W. Fu, D.Y. Liu, L.X. Chen, Magnetic molecularly imprinted microsensor for selective recognition and transport of fluorescent phycocyanin in seawater, J. Mater. Chem. A 3 (2015) 7437–7444.
[27] X.D. Zheng, J.M. Pan, L. Gao, X. Wei, J.D. Dai, W.D. Shi, Y.S. Yan, Silica nanoparticles doped with a europium(III) complex and coated with an ion imprinted polymer for rapid determination of copper(II), Microchim. Acta. 182 (2015) 753–761.
[28] R.X. Gao, X. Kong, X. Wang, X.W. He, L.X. Chen, Y.K. Zhang, Preparation and characterization of uniformly sized molecularly imprinted polymers functionalized with core–shell magnetic nanoparticles for the recognition and enrichment of protein, J. Mater. Chem 21 (2011) 17863–17871.
[29] M.S. Zhang, J.R. Huang, P. Yu, X. Chen, Preparation and characteristics of protein molecularly imprinted membranes on the surface of multiwalled carbon nanotubes, Talanta 81 (2010) 162–166.
[30] L. Qin, X.W. He, W. Zhang, W.Y. Li, Y.K. Zhang, Surface-modified polystyrene beads as photografting imprinted polymer matrix for chromatographic separation of proteins, J. Chromatogr. A 1216 (2009) 807–814.
[31] H.C. Chen, D.Y. Yuan, Y.Y. Li, M.J. Dong, Z.H. Chai, J. Kong, G.Q. Fu, Silica nanoparticle supported molecularly imprinted polymer layers with varied degrees of crosslinking for lysozyme recognition, Anal. Chim. Acta 779 (2013) 82–89.
[32] B. Deiminiat, I. Razavipanah, G.H. Rounaghi, M.H. Arbab-Zavar, A novel electrochemical imprinted sensor for acetylsalicylic acid based on polypyrrole, sol-gel and SiO_2@Au core-shell nanoparticles, Sens. Actuators B 244 (2017) 785–795.
[33] S.F. Xu, H.Z. Lu, Mesoporous structured MIPs@CDs fluorescence sensor for highly sensitive detection of TNT, Biosens. Bioelectron. 85 (2016) 950–956.
[34] L.X. Chen, X.Y. Wang, W.H. Lu, X.Q. Wu, J.H. Li, Molecular imprinting: perspectives and applications, Chem. Soc. Rev. 45 (2016) 2137–2211.
[35] X.Q. Wu, Z. Zhang, J.H. Li, H.Y. You, Y.B. Li, L.X. Chen, Molecularly imprinted polymers-coated gold nanoclusters for fluorescent detection of bisphenol A, Sens. Actuators B 211 (2015) 507–514.
[36] Z. Zhang, J.H. Li, X.Y. Wang, D.Z. Shen, L.X. Chen, Quantum dots based mesoporous structured imprinting microspheres for the sensitive fluorescent detection of phycocyanin, ACS Appl. Mater. Interfaces 7 (2015) 9118–9127.
[37] Z. Zhang, S.F. Xu, J.H. Li, H. Xiong, H.L. Peng, L.X. Chen, Selective solid-phase extraction of Sudan I in chilli sauce by single-hole hollow molecularly imprinted polymers, J. Agric. Food Chem. 60 (2012) 180–187.
[38] S.F. Xu, H.Z. Lu, Ratiometric fluorescence and mesoporous structure dual signal amplification for sensitive and selective detection of TNT based on MIP@QD fluorescence sensors, Chem. Commun. 51 (2015) 3200–3203.
[39] W.J. Yang, F.P. Jiao, L. Zhou, X.Q. Chen, X.Y. Jiang, Molecularly imprinted polymers coated on multi-walled carbon nanotubes through a simple indirect method for the determination of 2,4-dichlorophenoxyacetic acid in environmental water, Appl. Surf. Sci. 284 (2013) 692–699.
[40] Y.L. Liu, Y.H. He, Y.L. Jin, Y.Y. Huang, G.Q. Liu, R. Zhao, Preparation of monodispersed macroporous core-shell molecularly imprinted particles and their application in the determination of 2,4-dichlorophenoxyacetic acid, J. Chromatogr. A 1323 (2014) 11–17.
[41] H.J. Shi, G.H. Zhao, M.C. Liu, Z.L. Zhu, A novel photoelectrochemical sensor based on molecularly imprinted polymer modified TiO_2 nanotubes and its highly selective detection of 2,4-dichlorophenoxyacetic acid, Electrochem. Commun. 13 (2011) 1404–1407.
[42] K.P. Singh, S. Ahalawat, R.K. Prajapati, S. Kumar, P. Singh, D.S. Kumar, Electrochemical sensing for the detection of 2,4-dichlorophenoxy acetic acid using molecularly imprinted polymer membrane, Ionics 16 (2010) 529–537.
[43] C.G. Xie, S. Gao, Q.B. Guo, K. Xu, Electrochemical sensor for 2,4-dichlorophenoxy acetic acid using molecularly imprinted polypyrrole membrane as recognition element, Microchim. Acta 169 (2010) 145–152.
[44] S.A. Zhong, C.Y. Zhou, X.N. Zhang, H. Zhou, H. Li, X.H. Zhu, Y. Wang, A novel molecularly imprinted material based on magnetic halloysite nanotubes for rapid enrichment of 2,4-dichlorophenoxyacetic acid in water, J. Hazard. Mater. 276 (2014) 58–65.
[45] D.H. Peng, X. Li, L.Z. Zhang, J.M. Gong, Novel visible-light-responsive photoelectrochemical sensor of 2,4-dichlorophenoxyacetic acid using molecularly imprinted polymer/BiOI nanoflake arrays, Electrochem. Commun. 47 (2014) 9–12.
[46] S.M. Wang, L. Ge, L. Li, M. Yan, S.G. Ge, J.H. Yu, Molecularly imprinted polymer grafted paper-based multi-disk micro-disk plate for chemiluminescence detection of pesticide, Biosens. Bioelectron. 50 (2013) 262–268.

Biographies

Mengfan Jia received her bachelor degree in Food quality and safety from Northwest Agriculture & Forestry University, China, in 2015, and in the same year she joined Shaanxi Normal University, China. She is studying for her master degree. Her current research interest is molecularly imprinted polymers based chemical sensors for food and environmental analysis.

Zhong Zhang received his PhD degree from Yantai Institute of Coastal Zone Research, Chinese Academy of Sciences, China, in 2015. In the same year, he joined Shaanxi Normal University, China, as a lecturer. His current research interest focuses on the preparation of novel molecularly imprinted polymers and their applications in chemo/biosensors and chromatographic separation analysis.

Jinhua Li received her PhD in analytical chemistry from the Department of Chemistry of Hong Kong Baptist University, Hong Kong SAR, China, in 2009. In the same year, she joined Yantai Institute of Coastal Zone Research, Chinese Academy of Sciences, as an assistant professor. Now, she is an associate professor. Her current research interest focuses on preparation of novel molecularly imprinting polymers and their applications to sample pretreatment and chemosensing & biosensing.

Hongjun Shao received his PhD from Kunming institute of botany, Chinese academy of Sciences, in 2007. In the same year, he joined Shaanxi Normal University, China. Now he is an associate professor in Shaanxi Normal University. His current research interest focuses on separation of food component and food and chemical toxicology.

Lingxin Chen received his PhD degree in analytical chemistry from the Dalian Institute of Chemical Physics, Chinese Academy of Sciences, in 2003. After 2 years of postdoctoral experience at the Department of Chemistry, Tsinghua University, China, he joined first as a BK21 researcher and then as a research professor at the Department of Applied Chemistry, Hanyang University, Korea, in 2006. In 2009, as a professor, he joined Yantai Institute of Coastal Zone Research, Chinese Academy of Sciences. His research interests mainly include the studies of novel materials such as functionalization nanoparticles for developing nanometer biochemical analysis methods, and molecular imprinting technology.

Xingbin Yang received his PhD from Fourth Military Medical University, China, in 2004. He has engaged in food safety and nutrition research for many years, participated in many scientific research projects and published more than 80 SCI papers and his H-index is 18. Now he is a professor in Shaanxi Normal University. His research interest is mainly centered on food green processing and safety control.